Heliyon

ELSEVIER

Received:
16 December 2015
Revised:
1 February 2016
Accepted:
18 February 2016

Heliyon (2016) e00081

$LiCoPO_4$ cathode from a $CoHPO_4 \cdot xH_2O$ nanoplate precursor for high voltage Li-ion batteries

Daiwon Choi *, Xiaolin Li, Wesley A. Henderson, Qian Huang, Satish K. Nune, John P. Lemmon, Vincent L. Sprenkle

Energy and Environment Directorate, Pacific Northwest National Laboratory, Richland, WA99352, USA

* Corresponding author.

E-mail address: daiwon.choi@pnnl.gov (D. Choi).

Abstract

A highly crystalline $LiCoPO_4$/C cathode material has been synthesized without noticeable impurities via a single step solid-state reaction using $CoHPO_4 \cdot xH_2O$ nanoplate as a precursor obtained by a simple precipitation route. The $LiCoPO_4$/C cathode delivered a specific capacity of 125 $mAhg^{-1}$ at a charge/discharge rate of C/10. The nanoplate precursor and final $LiCoPO_4$/C cathode have been characterized using X-ray diffraction, thermogravimetric analysis – differential scanning calorimetry (TGA-DSC), transmission electron microscopy (TEM), and scanning electron microscopy (SEM) and the electrochemical cycling stability has been investigated using different electrolytes, additives and separators.

Keywords: Materials science, Nanomaterials, Materials synthesis, Materials chemistry, Alternative energy technologies

1. Introduction

Li-ion batteries – widely applied as an energy storage system of choice for electric vehicles, as well as for large scale stationary applications – have the highest energy density amongst the many types of proposed and commercialized

http://dx.doi.org/10.1016/j.heliyon.2016.e00081

2405-8440/© 2016 The Authors. Published by Elsevier Ltd. This is an open access article under the CC BY license (http://creativecommons.org/licenses/by/4.0/).

rechargeable batteries [1, 2, 3, 4, 5, 6]. Such a high energy density is attained, in part, by both the high specific capacity and voltage of the cathode electrode. Other than the conventionally used oxide-based cathodes, phosphate polyanion-type cathodes have been widely investigated. A notable example is the commercialization of $LiFePO_4$ which is one of the most stable cathode materials available due to its unique olivine structure [7, 8, 9, 10, 11, 12]. Among the olivine phosphate-based cathodes ($LiMPO_4$: M: Fe, Mn, Co and Ni), $LiCoPO_4$ possesses a high redox potential of 4.8 V *vs*. Li/Li^+, a flat voltage profile, and a high theoretical capacity of 167 $mAhg^{-1}$[13]. However, efforts to utilize $LiCoPO_4$ thus far have shown limited capacity and fast fading of the capacity upon repetitive cycles [13, 14, 15]. Like other phosphates, to access the full specific capacity from a $LiCoPO_4$ cathode, a nanostructured synthesis of the active material is desired [13, 16, 17, 18].

Various methods have been developed for $LiCoPO_4$ cathode synthesis including precipitation, hydrothermal, microwave, solid-state, mechanochemical, supercritical fluid and spray drying [14, 16, 17, 18, 19, 20, 21, 22, 23]. However, many of the synthesis routes reported are not suitable for scale-up and require complicated heat-treatment steps to ensure the formation of pure stoichiometric $LiCoPO_4$ since many of the available Co precursor can be easily reduced to form impurities such as Co metal, Co_3O_4 and Li_3PO_4 phases. Previously, NH_4CoPO_4 nanoplates were used as a starting material for $LiCoPO_4$, but multiple heat-treatments in both air and inert atmosphere were required to ensure formation of stoichiometric $LiCoPO_4$ since H_2 produced during the decomposition of NH_4CoPO_4 generates Co metal [14]. Other metal organic compounds are also prone to produce Co metal during heat-treatment by carbothermal reduction.

To form a stoichiometric $LiCoPO_4$ cathode without impurities, precursor compounds with strong Co-P bonding are desired. In the present work, a nanostructured $CoHPO_4{\cdot}xH_2O$ precursor was used to simplify the synthesis process and to minimize impurities. Previously, in related work, a $CoHPO_4{\cdot}3H_2O$ nanosheet electrode was hydrothermally synthesized for supercapacitors applications [24]. Finally, the effect of the electrolyte and separator on the cycling stability of the $LiCoPO_4$/C cathode obtained was investigated.

2. Experimental

The $LiCoPO_4$ cathode was synthesized by a solid-state reaction using LiOH, Ketjen black carbon (AkoNobel) and $CoHPO_4{\cdot}xH_2O$ nanoplate precursors. The $CoHPO_4{\cdot}xH_2O$ nanoplates were synthesized using a simple precipitation route from disodium pyrophosphate ($NaH_2P_2O_7$: Aldrich) and cobalt acetate tetrahydrate ($Co(CH_3COO)_2{\cdot}4H_2O$: Aldrich) in DI-water. Initially, 9.12 g of

http://dx.doi.org/10.1016/j.heliyon.2016.e00081
2405-8440/© 2016 The Authors. Published by Elsevier Ltd. This is an open access article under the CC BY license (http://creativecommons.org/licenses/by/4.0/).

ammonium acetate ($NH_4C_2H_3O_2$: Aldrich) and 8.18 g of $Na_2H_2P_2O_7$ were dissolved in 200 ml of DI-water, while 18.43 g of $Co(CH_3COO)_2{\cdot}4H_2O$ was dissolved separately in 100 ml of DI-water. The cobalt solution was slowly added to the disodium pyrophosphate solution while stirring and the pH of the mixture reached a value of 5 ~ 6. After the reaction proceeded for 8 h at 80 °C, the precipitated $CoHPO_4{\cdot}xH_2O$ was collected by centrifuging the solution and the solid was washed several times with DI-water and ethanol. The obtained $CoHPO_4{\cdot}xH_2O$ powder was dried at 80 °C in an oven for 2 days. The degree of hydration of the $CoHPO_4{\cdot}xH_2O$ was measured via TGA giving x equal to 1 (i.e., $CoHPO_4{\cdot}H_2O$) for the precursor dried at 80 °C in air. For the final $LiCoPO_4$/C cathode synthesis, the $CoHPO_4{\cdot}H_2O$ and LiOH (molar ratio 1:1) were mixed with 4.04 wt% (i.e., 5 wt% relative to $LiCoPO_4$) of Ketjen black using a planetary mill (Retch 200CM) for 4 h followed by heat-treatment in a tube furnace at 700 °C for 10 h under an UHP-Ar atmosphere with a heating rate of 5 °C min^{-1}.

A simultaneous differential scanning calorimetry (DSC) and thermogravimetric analysis (TGA) system (Netzsch STA 449C Jupiter) equipped with a SiC high temperature furnace (25–1550 °C) and a type-S sample holder was used to study the dehydration and phase transformation of the $CoHPO_4{\cdot}xH_2O$ nanoplate precursor. The powder sample was heated in an air environment up to 700 °C at a ramp rate of 5 °C min^{-1}. The crystal structure of the as-prepared $LiCoPO_4$/C composite was determined by X-ray diffraction (XRD) using a Rigaku Mini-Flex II with a CuKα sealed tube (λ = 1.54178 Å). All of the samples were scanned in a 2θ range between 5 to 80°, with a step size of 0.01° and an exposure time of 30 s. A JEOL 7001F scanning electron microscope (SEM) system was used to investigate the particle morphology. A high-resolution transmission electron microscopic (HRTEM) analysis was conducted using a FEI Tecnai G2 microscope with an acceleration voltage of 200 kV.

Electrodes were prepared by casting a slurry of the $LiCoPO_4$/C composite, acetylene black (MTI), and polyvinylidenedifluoride (PVDF, MTI) in *N*-methylpyrrolidone (NMP: Aldrich) solvent onto an Al foil current collector. The total weight percentage of carbon and PVDF in the electrode was 10 wt% (final weight ratio of $LiCoPO_4$: carbon: PVDF was 8:1:1). After drying at 120 °C overnight under vacuum, the electrodes were punched into 1.6 cm^2 disks. The active material loading was 1 ~ 2 mg cm^{-2}. Pure Li metal was used as an anode in a 2325 coin cell (NRC). The electrolyte consisted of 1 M $LiPF_6$ in a mixture of dimethyl carbonate (DMC) and ethylene carbonate (EC) (1:1 volume ratio) or DMC and fluoroethylene carbonate (FEC) (4:1 volume ratio) with 1.5 wt% of trimethylboroxine (TMB) additive. A Celgard 2500 or glassy microfiber (Whatman) separator was used. The coin cells were assembled in an Ar-filled MBraun glove box. The electrochemical tests were performed on

http://dx.doi.org/10.1016/j.heliyon.2016.e00081
2405-8440/© 2016 The Authors. Published by Elsevier Ltd. This is an open access article under the CC BY license (http://creativecommons.org/licenses/by/4.0/).

an Arbin BT-2000 battery cycler at room temperature. The cells were cycled between 3.0 and 5.2 V *vs.* Li/Li^+ at a C/10 (1C = 167 $mAhg^{-1}$) rate unless otherwise noted in the rate capability comparison.

3. Results and discussion

To synthesize the $LiCoPO_4$ nanoparticles, the $CoHPO_4{\cdot}xH_2O$ nanoplate precursor was obtained by a precipitation reaction between Co^{2+} and $P_2O_7{}^{4-}$ (from $Na_2H_2P_2O_7$) in acidic media of pH 5 ~ 6 at 80 °C for 8 h resulting in a violet $CoHPO_4{\cdot}xH_2O$ powder. Fig. 1(a, b) shows the powder XRD patterns of the as-prepared $CoHPO_4{\cdot}xH_2O$ precursor at different heat-treatment temperatures and the TGA-DSC analysis to determine the H_2O content up to 600 °C in air. All of the indexed peaks in the pattern are in agreement with $CoHPO_4{\cdot}3H_2O$ (JCPDS no. 39–0702) at 80 °C. No peaks of other phosphites or phosphates were detected from these patterns. The broad peaks indicate the presence of nanostructured or defected nature of the as-prepared $CoHPO_4{\cdot}xH_2O$ samples making them suitable for the final $LiCoPO_4$ nanoparticles with better electrochemical performance. The continuous dehydration of the samples upon increasing temperature resulted in a composition close to $CoHPO_4{\cdot}1.5H_2O$ (JCPDS no. 22–0222) at 200 °C followed by amorphization above 200 °C up to 500 °C in air. At 600 °C, the well-defined diffraction peaks (peak position and their relative intensities) were clearly observed and successfully indexed to the reflections of the monoclinic α-$Co_2P_2O_7$ crystal structure (JCPDS no. 49–1091) with a space group of $P2_1/c$ and cell parameters of a = 8.924, b = 8.366, and c = 9.016. Moreover, no other discernable diffraction reflections corresponding to other impurities (e.g., Co_2O_3, Co_3O_4, etc.) at 600 °C, indicating the Co/P ratio is 1/1 for the as-prepared $CoHPO_4{\cdot}xH_2O$ precursor.

For the subsequent stoichiometric $LiCoPO_4$ synthesis, an accurate determination of the H_2O content present in the as-prepared $CoHPO_4{\cdot}xH_2O$ precursor needed to be determined to calculate the stoichiometric amount of LiOH required. Therefore, a TGA-DSC analysis was performed on the as-prepared $CoHPO_4{\cdot}xH_2O$ where a 14.93 wt% decrease in weight was observed from 80 °C to 600 °C which is equivalent to x = 1 (15.63 wt% decrease) when a single $Co_2P_2O_7$ phase at 600 °C was used as a standard. The TGA result indicated a lower H_2O content (x = 1) than the XRD result where a crystal structure close to x = 3 was observed. The discrepancy between the XRD and TGA results for the hydration level of $CoHPO_4{\cdot}xH_2O$ is likely due to the creation of defects with a lower crystallinity thereby showing broader peaks since it has been reported that the dehydration of $CoHPO_4{\cdot}xH_2O$ ($0.5 \leq x \leq 1.5$) occurs almost isothermally which is sensitive to the synthesis temperature, drying condition, moisture level and synthesis time [25].

http://dx.doi.org/10.1016/j.heliyon.2016.e00081
2405-8440/© 2016 The Authors. Published by Elsevier Ltd. This is an open access article under the CC BY license (http://creativecommons.org/licenses/by/4.0/).

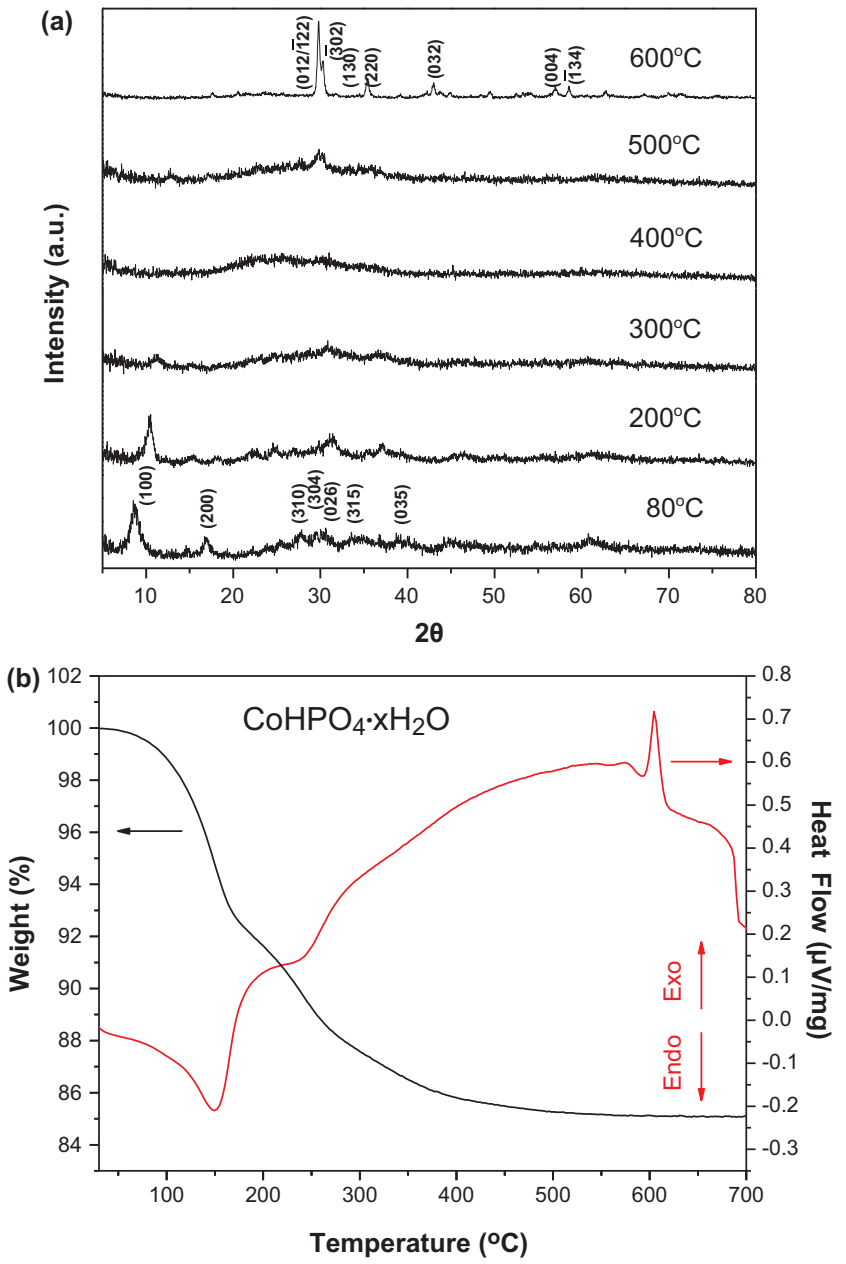

Fig. 1. (a) XRD patterns of the $CoHPO_4{\cdot}xH_2O$ nanoplate precursor at various temperatures in an air atmosphere and (b) TGA-DSC analysis of the $CoHPO_4{\cdot}xH_2O$ nanoplate precursor in an air atmosphere with a heating rate of 5 °C min^{-1}.

From both XRD and TGA studies, the crystalline $CoHPO_4{\cdot}H_2O$ dehydrates to amorphous $CoHPO_4$ as the temperature is increased above 200 °C. Between 200 °C and 500 °C, the amorphous $CoHPO_4$ slowly dehydrates to amorphous $Co_2P_2O_7$ before the start of crystallization above 590 °C. At 600 °C, β-$Co_2P_2O_7$ is the stable phase, but transforms to α-$Co_2P_2O_7$ as the temperature is decreased to room temperature [25, 26]. Overall, the dehydration and phase

http://dx.doi.org/10.1016/j.heliyon.2016.e00081
2405-8440/© 2016 The Authors. Published by Elsevier Ltd. This is an open access article under the CC BY license (http://creativecommons.org/licenses/by/4.0/).

evolution of the $CoHPO_4{\cdot}H_2O$ can be described as follows:

$$CoHPO_4{\cdot}H_2O \xrightarrow[-xH_2O]{\sim 200\,^{\circ}C} CoHPO_4{\cdot}0.2H_2O \xrightarrow[-xH_2O]{>250\,^{\circ}C} \text{amorphous } CoHPO_4 \xrightarrow[-H_2O]{>500\,^{\circ}C}$$

$$\text{amorphous } Co_2P_2O_7 \xrightarrow[\text{crystallization}]{>590\,^{\circ}C} \beta - Co_2P_2O_7 \xrightarrow[\text{reversible transformation}]{\sim 300\,^{\circ}C} \alpha - Co_2P_2O_7$$

Fig. 2 shows the SEM and TEM images of the as-prepared $CoHPO_4{\cdot}H_2O$ and the final $LiCoPO_4$/C obtained at 700 °C. A typical low-magnification TEM image in Fig. 2(a) shows a thin $CoHPO_4{\cdot}H_2O$ nanoplate morphology in the 2D microscale with 10 ~ 20 nm thickness and ~100 nm width and length. From the HRTEM image of the edge of a $CoHPO_4{\cdot}H_2O$ nanoplate comprised of ~20 single layers in Fig. 2(b), the measured distance of the neighboring lattice fringes was 10.63 nm which corresponds to the major (100) plane (interlayer spacing of 10.7 nm) of $CoHPO_4{\cdot}3H_2O$ indicating a layered structure for the $CoHPO_4{\cdot}H_2O$. The slightly lower spacing is probably due to a lower H_2O content from defects. In contrast, the synthesized final $LiCoPO_4$/C consists of spherical particles 100 ~ 400 nm in size covered with carbon. The $LiCoPO_4$ is obtained at 700 °C via the proposed reaction:

$$LiOH + CoHPO_4{\cdot}xH_2O \xrightarrow{\sim 700\,^{\circ}C} LiCoPO_4 + (1+x)\,H_2O\uparrow$$

The layered structure of the $CoHPO_4{\cdot}xH_2O$ nanoplates and the amorphization at elevated temperature facilitate the Li diffusion into the $CoHPO_4{\cdot}xH_2O$ matrix

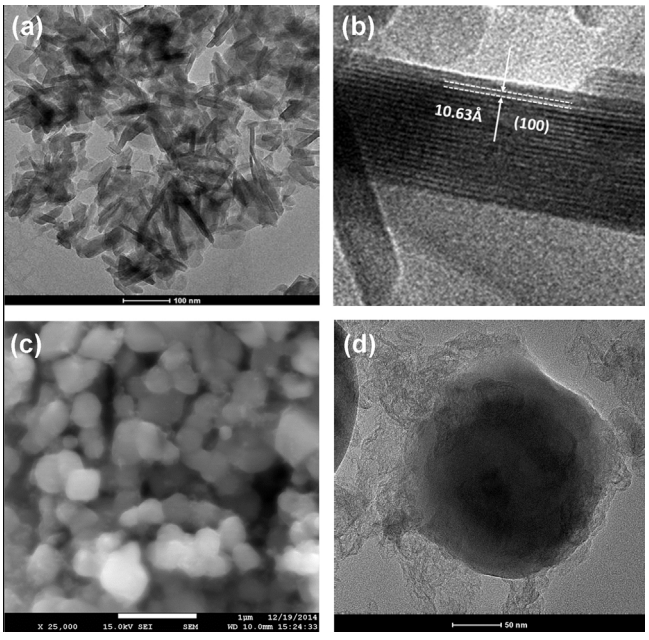

Fig. 2. High-resolution (a, b) TEM images of the synthesized $CoHPO_4{\cdot}H_2O$ nanoplate precursor, (c) SEM and (d) TEM images of the $LiCoPO_4$/C synthesized at 700 °C under an UHP-Ar atmosphere.

http://dx.doi.org/10.1016/j.heliyon.2016.e00081
2405-8440/© 2016 The Authors. Published by Elsevier Ltd. This is an open access article under the CC BY license (http://creativecommons.org/licenses/by/4.0/).

with only H_2O as a by-product resulting in uniform nanoparticles without much grain growth.

Fig. 3 shows the Rietveld refinement of the XRD pattern of the $LiCoPO_4$/C nanocomposite based on the orthorhombic *Pnma* space group where the *b* and *a* axes were switched from *Pnmb* (JCPDS No. 33–0804), which is isostructural to $LiCoPO_4$. The refined lattice parameter matches closely that of pure orthorhombic $LiCoPO_4$ (*Pnma*, a = 10.212, b = 5.927, c = 4.705 Å). Moreover, no other discernable diffraction reflections were evident corresponding to other impurities known to be present from heat-treatment with carbon during $LiCoPO_4$/C synthesis, indicating the stoichiometric nature of the $CoHPO_4 \cdot H_2O$ nanoplate precursor.

Fig. 4(a) shows the voltage profiles of the $LiCoPO_4$/C cathode for various discharge rates. At a C/10 rate, a specific capacity of 125 $mAhg^{-1}$ was observed and at a 1C rate, a specific capacity of > 80 $mAhg^{-1}$ was achieved. The rate performance of $LiCoPO_4$ is better than that of a $LiMnPO_4$ cathode [8].

While the high voltage $LiCoPO_4$ cathode delivers an acceptable capacity and rate performance without the need of excessive conductive carbon (as is done for a $LiMnPO_4$ cathode), $LiCoPO_4$ has been reported to have a fast fade in capacity upon electrochemical cycling which limits its application. Numerous reports on the origin of the poor cycling stability of $LiCoPO_4$ indicate that the fast capacity fading in $LiPF_6$ containing electrolyte solutions is believed to be due to the nucleophilic attack of the HF (always) present in these electrolyte on the P atoms of the olivine compound in the delithiated state resulting in the formation of soluble PO_3F^{2-}, $PO_2F_2^-$, POF_3 and H_2O. The H_2O produced then reacts with PF_6^-, POF_3 and $PO_2F_2^-$ to produce more HF [15, 27]. Therefore,

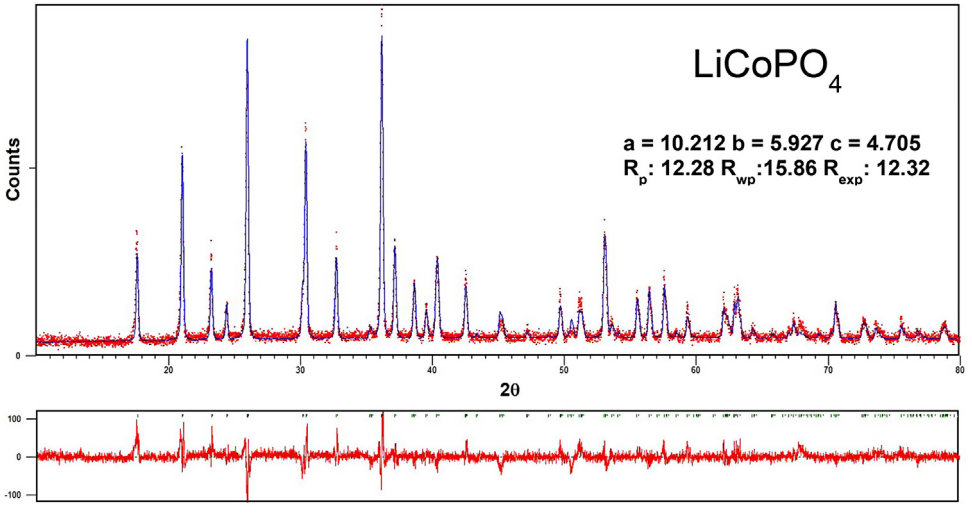

Fig. 3. Rietveld refinement of the XRD pattern of the $LiCoPO_4$/C cathode.

http://dx.doi.org/10.1016/j.heliyon.2016.e00081
2405-8440/© 2016 The Authors. Published by Elsevier Ltd. This is an open access article under the CC BY license (http://creativecommons.org/licenses/by/4.0/).

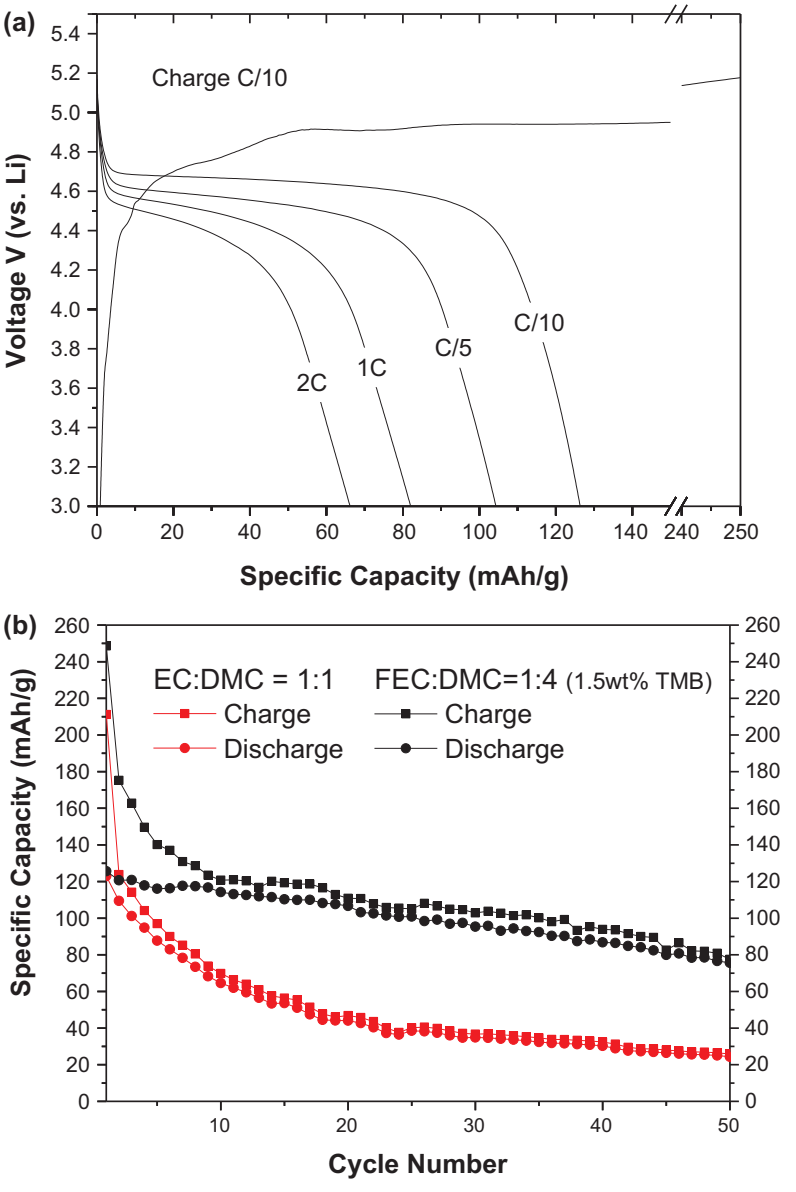

Fig. 4. (a) Electrochemical charge–discharge curves at various C-rates and (b) cycling performance of the $LiCoPO_4$/C cathode using different electrolytes and separators at a C/10 charge-discharge rate.

to prevent $CoPO_4$ dissolution during cycling, HF should ideally be eliminated – which is a challenging task. Various strategies have been tested to stabilize the cycling performance including the use of an HF scavenging separator, protective coating, and doping to induce SEI (solid electrolyte interphase) layer formation using electrolyte additives [15, 28]. Using the latter approach, Fe-substituted $LiCoPO_4$ exhibited an improved cycling stability due to the stabilization of the structure in the delithiated state [29, 30]. However, a lower specific capacity was achieved when Fe was used as a dopant. Recently,

http://dx.doi.org/10.1016/j.heliyon.2016.e00081
2405-8440/© 2016 The Authors. Published by Elsevier Ltd. This is an open access article under the CC BY license (http://creativecommons.org/licenses/by/4.0/).

various electrolyte additives have also improved the cycling performance. An improved capacity retention was observed when $LiCoPO_4$ was cycled with an electrolyte containing either tris(hexafluoroisopropyl) phosphate (HFiP) or trimethylboroxine (TMB) [31]. Additionally, the use of alternative separators such as glassy paper or quartz has increased the cycling stability relative to the conventional polyethylene(PE)/polypropylene (PP) separators due to the presence of silica, which is known to be a HF scavenger.

The cyclic performance of the $LiCoPO_4$/C cathode is shown in Fig. 4(b). The large irreversible losses in the capacities observed at the beginning of the cycles are believed to be due to the SEI layer formation by the decomposition of the electrolyte and the additives. When a conventional 1 M $LiPF_6$ in EC:DMC (1:1 v/v) electrolyte was used, ~50% and ~80% degradation in the specific capacity after 10 and 50 cycles has been observed, respectively, which is similar to previous reports [14, 28]. However, when a glassy separator and a 1 M $LiPF_6$ in FEC:DMC (1:4 v/v) electrolyte with 1.5 wt% TMB additive was used, over 90% and 60% of the initial capacity has been retained after 10 and 50 cycles, respectively. The FEC-based electrolyte with the TMB additive demonstrates a dramatic improvement in the cycling characteristics of the $LiCoPO_4$/Li cells as compared to the EC-based electrolyte. Achieving an electrolyte with high voltage stability and HF minimization is a challenging task. Further investigations on the cycling stability of the cathode are currently ongoing and detailed information regarding the influence of the electrolyte formulations on the $LiCoPO_4$ cycling stability will be reported in the future.

4. Conclusions

A highly stoichiometric $LiCoPO_4$/C cathode material has been synthesized using a $CoHPO_4{\cdot}xH_2O$ precursor obtained by a simple precipitation route at room temperature which is suitable for a large scale synthesis. The $CoHPO_4{\cdot}xH_2O$ obtained has a nanoplate shape morphology with a $x = 1$ hydration level. A pure, stoichiometric $LiCoPO_4$/C cathode was obtained by a single step heat-treatment at 700 °C which delivers a specific capacity of 125 $mAhg^{-1}$ at a C/10 rate containing 10 wt% conductive carbon additive indicating that the $CoHPO_4{\cdot}xH_2O$ precursor is an ideal starting material for $LiCoPO_4$ cathode synthesis. With a variation in the composition of a carbonate-based electrolyte and use of an additive, a significant improvement in the cycling stability was observed. It is likely that, with a more systematic understanding of the degradation mechanism(s) and further electrolyte optimization, the cycling performance of the high voltage $LiCoPO_4$ cathode can be significantly improved.

http://dx.doi.org/10.1016/j.heliyon.2016.e00081
2405-8440/© 2016 The Authors. Published by Elsevier Ltd. This is an open access article under the CC BY license (http://creativecommons.org/licenses/by/4.0/).

Declarations

Author contribution statement

Daiwon Choi: Conceived and designed the experiments; Wrote the paper.

Daiwon Choi, Qian Huang, Wesley A. Henderson, Xiaolin Li: Performed the experiments.

Daiwon Choi, Satish K. Nune: Analyzed and interpreted the data.

John P. Lemmon, Vincent L. Sprenkle: Contributed reagents, materials, analysis tools or data.

Funding statement

This work was supported by the U.S. Department of Energy's (DOE's) Office of Electricity Delivery and Energy Reliability (OE) (under Contract No. 57558).

Competing interest statement

The authors declare no conflict of interest.

Additional information

No additional information is available for this paper.

Acknowledgements

PNNL is a multi-program national laboratory operated by Battelle for the DOE under Contract DE-AC05–76RL01830.

References

[1] Z. Yang, et al., Electrochemical energy storage for green grid, Chem. Rev. 111 (5) (2011) 3577–3613.

[2] T. Xu, et al., Lithium-ion batteries for stationary energy storage, JOM 62 (9) (2010) 24–30.

[3] J. Cho, S. Jeong, Y. Kim, Commercial and research battery technologies for electrical energy storage applications, Prog. Energ. Combust. 48 (2015) 84–101.

[4] H. Chen, et al., Progress in electrical energy storage system: A critical review, Prog. Nat. Sci. 19 (3) (2009) 291–312.

[5] Q. Huang, et al., Composite organic radical–inorganic hybrid cathode for lithium-ion batteries, J.Power Sources 233 (2013) 69–73.

 http://dx.doi.org/10.1016/j.heliyon.2016.e00081

2405-8440/© 2016 The Authors. Published by Elsevier Ltd. This is an open access article under the CC BY license (http://creativecommons.org/licenses/by/4.0/).

[6] Q. Huang, et al., Multi-electron redox reaction of an organic radical cathode induced by a mesopore carbon network with nitroxide polymers, Phys. Chem. Chem. Phys. 15 (48) (2013) 20921–20928.

[7] W. Wang, D. Choi, Z. Yang, Li-ion battery with $LiFePO_4$ cathode and $Li_4Ti_5O_{12}$ anode for stationary energy storage, Metall. Mater. Trans. A 44 (1) (2013) 21–25.

[8] D. Choi, et al., $LiMnPO_4$ nanoplate grown via solid-state reaction in molten hydrocarbon for Li-ion battery cathode, Nano Letters 10 (8) (2010) 2799–2805.

[9] D. Choi, et al., Thermal stability and phase transformation of electrochemically charged/discharged $LiMnPO_4$ cathode for Li-ion batteries, Energy Environ. Sci. 4 (11) (2011) 4560–4566.

[10] Z. Gong, Y. Yang, Recent advances in the research of polyanion-type cathode materials for Li-ion batteries, Energy Environ. Sci. 4 (9) (2011) 3223–3242.

[11] A. Yamada, S.C. Chung, K. Hinokuma, Optimized $LiFePO_4$ for lithium battery cathodes, J. Electrochem. Soc. 148 (3) (2001) A224–A229.

[12] A.K. Padhi, K.S. Nanjundaswamy, J.B. Goodenough, Phospho-olivines as positive-electrode materials for rechargeable lithium batteries, J. Electrochem. Soc. 144 (4) (1997) 1188–1194.

[13] B. Sergio, P. Stefania, Recent advances in the development of $LiCoPO_4$ as high voltage cathode material for Li-ion batteries in nanotechnology for sustainable energy, J. Am. Chem. Soc. (2013) 67–99.

[14] S.-M. Oh, S.-T. Myung, Y.-K. Sun, Olivine $LiCoPO_4$-carbon composite showing high rechargeable capacity, J. Mater. Chem. 22 (30) (2012) 14932–14937.

[15] E. Markevich, et al., Reasons for capacity fading of $LiCoPO_4$ cathodes in $LiPF_6$ containing electrolyte solutions, Electrochem. Commun. 15 (1) (2012) 22–25.

[16] K. Amine, H. Yasuda, M. Yamachi, Olivine $LiCoPO_4$ as 4.8 V electrode material for lithium batteries, Electrochem. Solid State Lett. 3 (4) (2000) 178–179.

[17] J. Liu, et al., Spherical nanoporous $LiCoPO_4$/C composites as high performance cathode materials for rechargeable lithium-ion batteries, J. Mater. Chem. 21 (27) (2011) 9984–9987.

 http://dx.doi.org/10.1016/j.heliyon.2016.e00081

2405-8440/© 2016 The Authors. Published by Elsevier Ltd. This is an open access article under the CC BY license (http://creativecommons.org/licenses/by/4.0/).

[18] Q.D. Truong, et al., Controlling the shape of $LiCoPO_4$ nanocrystals by supercritical fluid process for enhanced energy storage properties, Sci. Rep. 4 (2014) 3975.

[19] H.H. Li, et al., Fast synthesis of core-shell $LiCoPO_4$/C nanocomposite via microwave heating and its electrochemical Li intercalation performances, Electrochem. Commun. 11 (1) (2009) 95–98.

[20] J. Yoshida, S. Nakanishi, H. Iba, Improvement of battery performances of $LiCoPO_4$ as cathode material for lithium ion batteries, Meeting Abstracts MA2012-02 (10) (2012) 796.

[21] M. Kotobuki, Hydrothermal synthesis of carbon-coated $LiCoPO_4$ cathode material from various Co sources, IJEEE 4 (1) (2013) 25.

[22] K. Dokko, S. Koizumi, K. Koizumi, Electrochemical reactivity of $LiFePO_4$ prepared by hydrothermal method, Chem. Lett. 35 (2006) 338.

[23] K. Dokko, et al., Electrochemical properties of $LiFePO_4$ prepared via hydrothermal route, J. Power Sources 165 (2007) 656–659.

[24] H. Pang, et al., Few-layered $CoHPO_4{\cdot}3H_2O$ ultrathin nanosheets for high performance of electrode materials for supercapacitors, Nanoscale 5 (13) (2013) 5752–5757.

[25] D. Brandová, et al., Mechanism of the dehydration of $CoHPO_4 \cdot 1.5H_2O$, J. Thermal Anal. 34 (3) (1988) 673–678.

[26] K. Hashimoto, et al., Property of spherical cobalt hydrogenphosphate hydrate, Gypsum & Lime 1990 (228) (1990) 277–284.

[27] D. Aurbach, Cycling performance of $LiCoPO_4$ cathodes: reasons for capacity fading and effect of the electrolyte composition, Meeting Abstracts MA2013-02(14) (2013) 997.

[28] R. Sharabi, et al., Significantly improved cycling performance of $LiCoPO_4$ cathodes, Electrochem. Commun. 13 (8) (2011) 800–802.

[29] D.-W. Han, et al., Effects of Fe doping on the electrochemical performance of $LiCoPO_4$/C composites for high power-density cathode materials, Electrochem. Commun. 11 (1) (2009) 137–140.

[30] S.M.G. Yang, et al., Realizing the performance of $LiCoPO_4$ cathodes by Fe substitution with off-stoichiometry, J. Electrochem. Soc. 159 (7) (2012) A1013–A1018.

[31] A. von Cresce, K. Xu, Electrolyte additive in support of 5 V Li ion chemistry, J. Electrochem. Soc. 158 (3) (2011) A337–A342.

 http://dx.doi.org/10.1016/j.heliyon.2016.e00081

2405-8440/© 2016 The Authors. Published by Elsevier Ltd. This is an open access article under the CC BY license (http://creativecommons.org/licenses/by/4.0/).